P7.6 Validation of Goes-9 Satellite-Derived Cloud Properties over the Tropical Western Pacific Region

Mandana M. Khaiyer*, Michele L. Nordeen, David.R.Doelling, Venkatasan Chakrapani
Analytical Services & Materials Inc., Hampton, VA

Patrick Minnis, William L. Smith, Jr.
Atmospheric Sciences, NASA-Langley Research Center, Hampton, VA

1. INTRODUCTION

Whereas ground-based instruments can provide valuable climatological information, they are available only over small portions of the Earth's surface. More expansive data coverage is essential to studying and understanding the Earth's climate. Towards this end, satellite coverage can fill in large gaps where surface-based instruments are unavailable.

One climatically important region with a relative paucity of ground-based instruments is the Tropical Western Pacific (TWP). This region, covering 10°N – 10°S and 120°E to 150°W, has been selected by the Atmospheric Radiation Measurement (ARM) Program as one of its three long-term study regions. Within the larger domain, three sites at Manus Island (2.0°S, 147.4 °E), Nauru Island (0.5°S 166.9°E), and Darwin, AUS (12.4°S 130.9°E) have been selected by ARM as the locations for a suite of ground-based instruments to study cloud and radiative properties. In order to provide additional climatological coverage of the TWP region over a larger scale, the ninth Geostationary Operational Environmental Satellite (GOES-9) is employed to derive cloud and radiation characteristics for the region.

Real-time processing of hourly GOES-9 images in the ARM TWP region began operationally in October 2003 and is continuing. The ARM sites provide an excellent source for validating this new satellite-derived cloud and radiation property dataset. Derived cloud amounts, heights, and broadband shortwave fluxes are compared with similar quantities derived from ground-based instrumentation. The results will provide guidance for estimating uncertainties in the GOES-9 products and to develop improvements in the retrieval methodologies and input.

2. METHODOLOGY

The GOES-9 data are taken hourly with a nominal pixel resolution of 4 km. However, because of significant noise in the GOES-9 visible (0.65 µm) channel, 1-km visible pixel radiances are averaged into 4-km pixels. Results from Nguyen et al. (2004) were used to calibrate the GOES-9 visible-channel data. Daytime data are analyzed with the visible infrared solar-infrared split-window technique (VISST), which is an updated version of the methodology described by Minnis et al. (1995b). First, each pixel is classified as clear or cloudy using the algorithms described by Trepte et al. (1999), which use data from the 0.65,3.9, 10.8, and 12.0 µm channels. The same radiances are used by the VISST to estimate cloud phase, effective temperature *Tc*, effective height, optical depth, effective particle size, and liquid or ice water path for each cloudy pixel. Cloud-top height and thickness are also derived using empirical methods (Minnis et al. 1990, Chakrapani et al. 2001). At night and near the terminator, all times when the solar zenith angle SZA > 82°, the visible channel is unusable, so the cloud height and temperature and a crude estimate of optical depth are estimated using an updated version of the solar-infrared infrared split-window technique (SIST; Minnis et al. 1995b). This paper focuses only on daytime results. GOES-9 and VISST are used interchangeably to denote any retrievals from GOES-9. VISST retrievals were performed on GOES-9 data over the expanded TWP domain (10°N - 20°S, 120°E - 180°) on a real-time basis from October 2003 through the present. These retrievals used the Global Forecasting Systems Aviation (AVN) model output to provide vertical profiles of temperature and humidity; such profiles are necessary to correct for atmospheric attenuation of the radiances, and to estimate the cloud height from *Tc*. Regional retrievals, using Meteorological Ozone and Aerosol atmospheric profiles from the Clouds and Earth's Radiant Energy System (CERES; see Wielicki et al. 1998), were performed for 1° areas over the three ARM sites at Manus, Nauru, and Darwin from April 16- September 30, 2003.

The datasets used for validation include retrievals and image products from available ARM instruments at Manus, Nauru, and Darwin. These include the Millimeter Cloud Radar (MMCR), total sky imagers (TSI), the MicroPulse Lidar (MPL), and ceilometers. The comparisons utilize cloud amounts and cloud top heights derived using the Active Remote Sensing of Cloud Layers (ARSCL) methods (Clothiaux et al. 2000). VISST cloud amounts and heights were averaged over all pixels within a 20-km radius of the site; these "instantaneous" values are compared with 20-min averages of TSI cloud amounts and ARSCL cloud boundary data centered on the GOES-9 retrieval times. Averages were computed for all retrievals with SZA < 80°.

For the TSI data, averages are based on "percent opaque" plus "percent thin" data within the 20 minute window. Cloud fraction from the ARSCL data is defined as the number of cloud occurrences divided by the total number of observations during the 20-min period. Since the ARSCL data is provided in 10 layers, the cloud amount was derived per layer. As with GOES9

* *Corresponding Author Address*: Mandana M. Khaiyer, AS&M, Inc., 1 Enterprise Parkway Hampton, VA 23666;
E-mail: m.m.khaiyer@larc.nasa.gov.

retrievals, average cloud amounts for ARSCL and TSI were both computed only for SZA < 80°. In order to

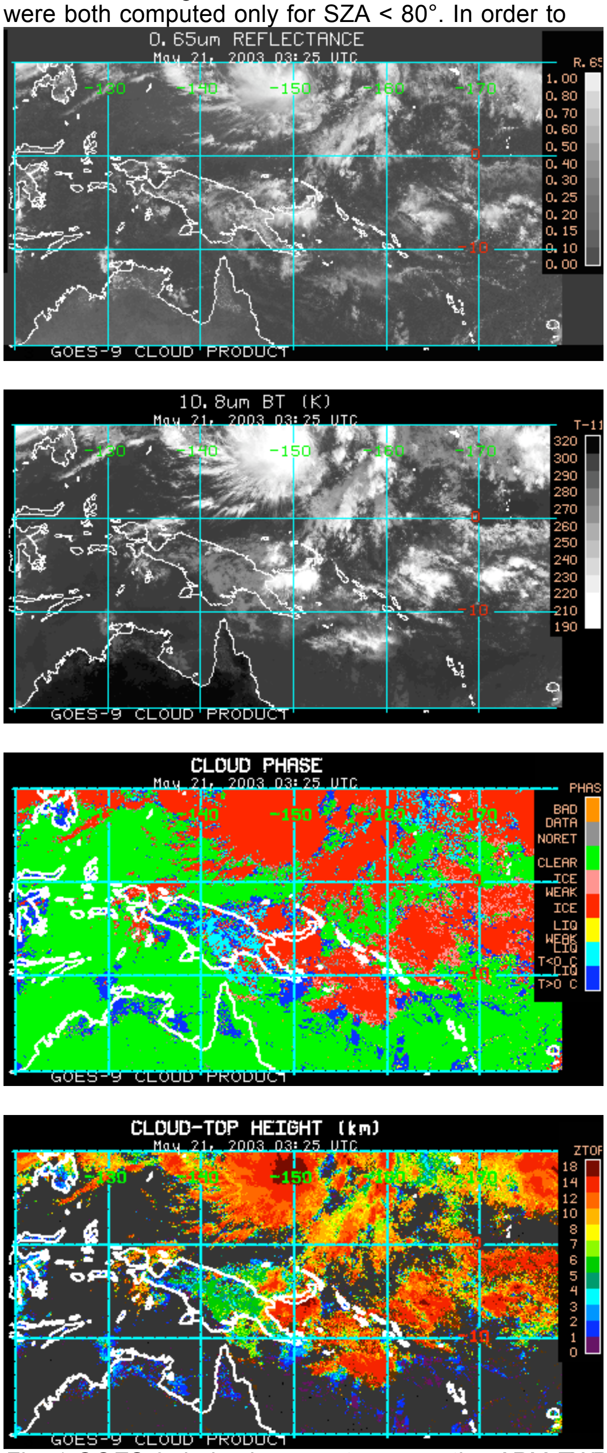

Fig. 1 GOES-9 derived parameters over the ARM TWP domain for 0218 UTC May 1, 2003. (a) 0.63-μm reflectance (b) 10.8-μm brightness temperature, (c) cloud phase, (d) cloud top height (μm).

compute an average for a particular day, a minimum of 4 hourly retrievals from GOES9 were required. Corresponding TSI daily averages were computed for all cloud fraction observations taken at SZA < 80°. The largest cloud amount within the ARSCL layers was taken as the ARSCL-derived cloud amount for use in daily averages, which is likely to lead to a low bias in broken cloud multi-level cases. For this reason, only single-layer ARSCL cases were compared for specific 20 minute-averaged values.

Broadband shortwave albedos derived from the CERES scanner on the *Terra* satellite were used to validate the GOES-derived albedos. ERBE-like albedos derived from CERES pixels with centers falling within the GOES-9 circles around the ARM sites were averaged during a given *Terra* overpass for comparison with the albedos derived from the GOES-9 narrowband data during April-August 2003.

3. RESULTS

GOES-9 visible and infrared imagery as well as cloud phase and cloud-top height retrievals from VISST are shown in Fig. 1 for data taken at at 0325 UTC May 21, 2003. The cloud features, including cirrus outflow from a storm centered at about 4°N 148°E, are fairly well-resolved in the cloud phase field (Fig. 1c). Cloud heights for this feature are in the 12 – 18 km range, consistent with tropical cirrus anvils (Fig. 1d).

For the purposes of showing general trends in daily-averaged cloud amounts, Figs. 2-4 show the GOES-9 daily daytime cloud amount versus the available TSI- and ARSCL-derived cloud amounts averaged over the same time periods. The Darwin TSI (blue) and GOES9 (red) daily averaged cloud amounts (Figs. 2a, b) track each other quite well on a day-to-day basis. The wintertime trend in Fig 2a shows lower cloud amounts than seen in the monsoonal conditions reflected in the summertime plot (Fig. 2b); the average GOES9 (TSI) cloud amount for winter conditions is 24.2% (19.5%), versus 87.3% (82.8%) in summer. The scatterplot in Fig. 2c reflects the consistency indicating that the GOES-9 cloud amount never drops to zero yielding a bias of a few percent when the TSI cloud amount is zero. At Nauru (Fig. 3a), the ARSCL cloud amounts are generally smaller than the TSI values except when GOES-9 detects very small cloud amounts (Fig. 3b). Then, both surface instruments detect cloud amounts of ~ 25% compared to 3 or 4% from GOES-9. One noticeable result in the scatterplot is that the ARSCL yields an average cloud amount of ~ 65% when both the TSI and GOES-9 amounts are greater than 90%. This is probably due to a possible low bias introduced in broken cloud multi-level cases, due to the methodology employed here when deriving daily cloud amounts from ARSCL. To eliminate this possible discrepancy, only single-level cases will be used for further 20-minute average comparisons. This discrepancy can also be noted in the Manus comparison (Fig. 4). A comparison of ARSCL-derived daily cloud averages versus GOES9 values over Manus (Fig. 4a) shows a similar trend, with a number of cases where GOES9 detects 100% cloud, and ARSCL detects less (Fig. 4b).

The mean for the daily daytime averaged GOES-9 minus TSI difference in Darwin, for available cases between April 2003- July 2004, is 0.7% with a RMS difference of 11.7%. At Nauru, the GOES9 – TSI bias for cases between May – December 2003 was –7.3%

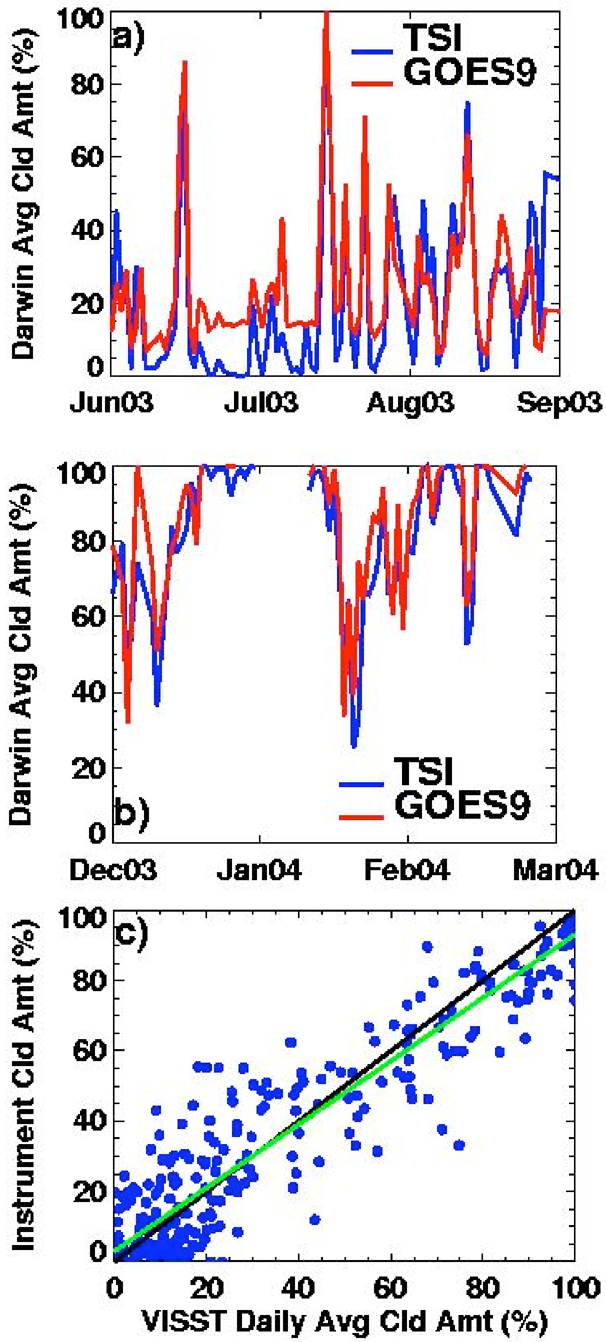

Fig. 2 Comparisons of daily daytime averaged cloud amounts over Darwin, AUS, for VISST vs TSI, for (a) wintertime, (b) summertime, (c) a scatterplot comparison of all available data from April 2003-July 2004.

with an RMS difference of 21.8%. For the same region but for the time period, May-August 2003, the GOES-9 cloud amount averages 0.8% more than the ARSCL value with a 25.2% rms difference. For Manus, the GOES9 – ARSCL difference for April through September 2003 is 9.5%, with an RMS difference of 23.5%.

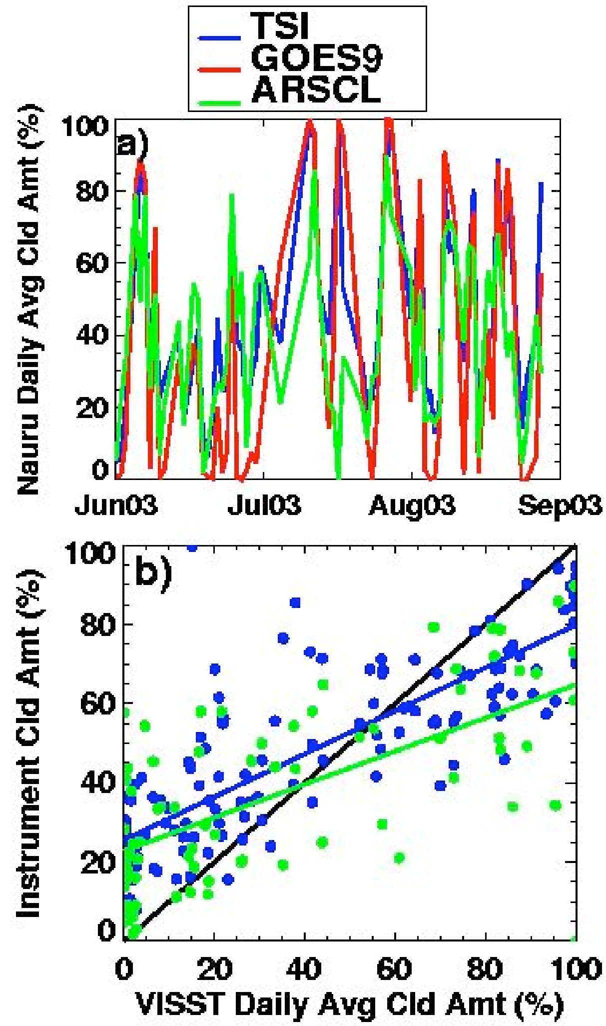

Fig. 3 Comparisons of daily daytime averaged cloud amounts over Nauru, for VISST vs TSI, and VISST vs ARSCL, for (a) wintertime, (b) a scatterplot comparison of all available data from May – December 2003. Blue dots denote VISST vs TSI for May-December 2003, and green dots denote VISST vs ARSCL comparison for April-August 2003. Blue and green lines correspond to line fits for the data types, and black indicates the one-to-one correlation line.

Figure 5 shows scatterplots of the CERES ERBE-like broadband shortwave albedo versus their narrowband-based GOES-9 values. In general, the albedos are fairly well-correlated. On average, the GOES-9 minus CERES albedo differences are -0.015 for Manus (Fig. 5a), -0.005 for Nauru (Fig. 5b), and 0.003 for Darwin (Figure 5c). The corresponding RMS differences are 0.113, 0.037, and 0.029, respectively. Since cloud amounts during the April - August time frame are typically larger at Manus than at Darwin or Nauru, the greater range and scatter of the data are expected at Manus.

Comparisons were also performed using the individual VISST 20-km radius cloud fraction and the

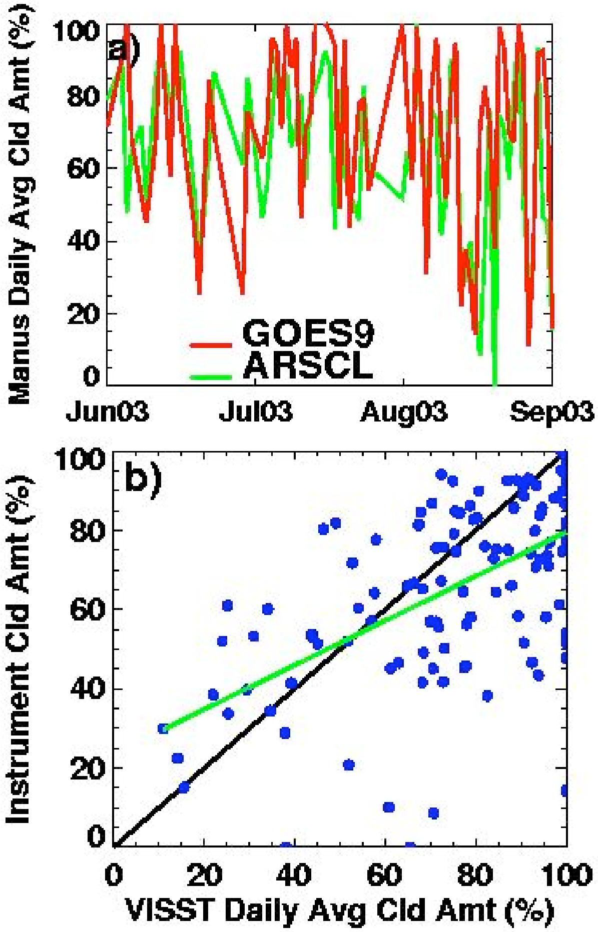

Fig. 4 Comparisons of daily daytime averaged cloud amounts over Manus, for VISST vs ARSCL, for (a) wintertime, (b) a scatterplot comparison of all available data from April – September 2003. Blue dots denote VISST vs ARSCL comparison for April-September 2003. The green line corresponds to the line fits for the data, and black indicates the one-to-one correlation line.

20-minute averaged cloud fractions derived from TSI and ARSCL. The cloud amounts derived by the various methods are placed into four bins: 0-20%, 20-50%, 50-80%, and 80- 100%. Values along the diagonal indicate that both methods agree to within the bin limits.

For Darwin in winter (Table 1a), TSI and VISST agree in 71% of all cases, with 58% of the cases being in the 0-20% bin. The most obvious error class is GOES-9 overestimating TSI's 0-20% binned cloud amounts into higher cloud amount bins, in 14% of cases. This trend can also be seen in the daily average comparisons (Figure 2a). The TSI average cloud amount is 19.7% compared to 24.1% from VISST, yielding a bias of 4.4% and an RMS difference of 25.0%. For summer in Darwin (Table 1b), TSI and GOES-9 VISST agree in 77% of cases, with no large error classes. The average cloud amount for TSI during this time period is 82.1% versus 86.8% for

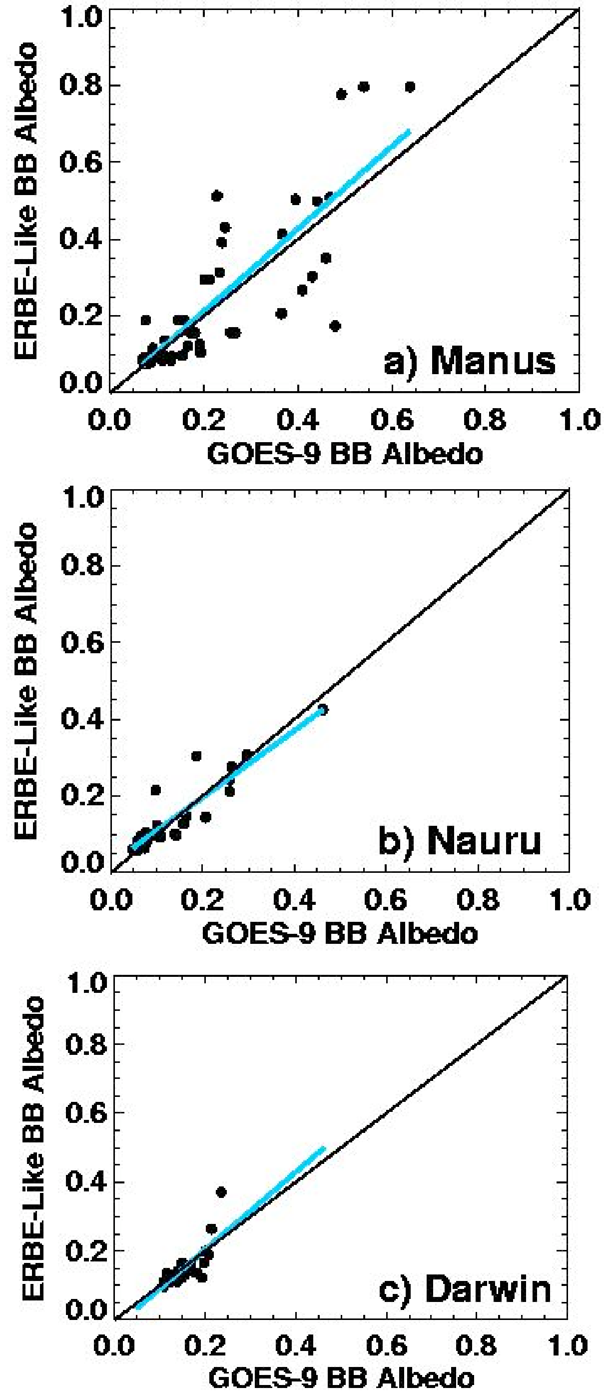

Fig. 5 Comparisons of GOES9 versus ERBE-Like broadband albedoes from(a) Manus, (b) Nauru, and (c) Darwin.Teal denotes the line fit to the data, and black the one-to-one agreement line.

VISST, leading to a bias of 4.7% and an RMS difference of 18.7%. For all available cases at Darwin (Table 1c), which included 3068 samples between April 2003- July 2004, the cloud classes agreed 66% of time. The overall bias was 2.1% (42.7% average for

VISST versus 40.6% for TSI) yielding an RMS difference of 32.4%.

Table 1a. VISST vs TSI binned cloud amounts for Darwin, June-Aug. 2003.

	VISST				
	CF(%)	0-20	20-50	50-80	80-100
TSI	80-100	1	1	2	6
	50-80	1	4	3	1
	20-50	3	4	2	1
	0 -20	58	9	2	3

Table 1b. Same as 1a, for Dec. 2003-Feb. 2004.

	VISST				
	CF(%)	0-20	20-50	50-80	80-100
TSI	80-100	0	1	2	67
	50-80	0	2	3	9
	20-50	1	4	2	4
	0 -20	3	1	1	0

Table 1c. Same as 1a, for Apr. 2003-July 2004.

	VISST				
	CF(%)	0-20	20-50	50-80	80-100
TSI	80-100	2	1	2	22
	50-80	1	3	3	4
	20-50	5	4	2	2
	0 -20	37	5	3	4

A comparison of VISST and TSI cloud fractions was also completed for the Nauru site (Table 2). For the months of June-August 2003 (Table 2a), the sources agree in 57% of the cases. VISST's average cloud amount is 42.6% compared to 46.1% for TSI, leading to a bias of -3.7% and an RMS difference of 23.9%. Table 2b shows the results of all matches between May-December 2003 at Nauru, which agree in 56% of the cases. For 1576 cases, the bias is –4.4%, reflecting an average cloud amount of 47.2% for TSI and 42.8% for VISST. The corresponding RMS difference is 24.4%.

There were very few TSI data available for comparison with VISST at Manus, so a limited comparison for the November 2003- January 2004 was made (Table 3). Of the 153 cases, 67% fall in the same cloud amount bin. The average cloud amount for TSI is 69.4% compared to 79.4% for VISST, leading to a bias of 10.0% and an RMS difference of 22.7%.

A comparison of daytime ARSCL and GOES-9 cloud properties was also performed for Nauru and Manus (not shown). For these comparisons, only ARSCL-defined single-layer cases were used. At Nauru, VISST and ARSCL agree 46% of the time, with the most common error classes corresponding to ARSCL 20-50% and VISST 0-20% coverage,

Table 2a. VISST vs TSI binned cloud amounts for Nauru, Jun03-Aug03.

	VISST				
	CF(%)	0-20	20-50	50-80	80-100
TSI	80-100	0	1	1	22
	50-80	4	2	4	7
	20-50	18	6	3	2
	0 -20	25	3	1	1

Table 2b. Same as 2b, May 2003- December 2003.

	VISST				
	CF(%)	0-20	20-50	50-80	80-100
TSI	80-100	0	0	2	22
	50-80	4	3	4	7
	20-50	18	7	4	2
	0 -20	23	3	1	0

Table 3. VISST vs TSI cloud amounts for Manus, November 2003- January 2004.

	VISST				
	CF(%)	0-20	20-50	50-80	80-100
TSI	80-100	0	0	0	54
	50-80	0	1	3	11
	20-50	7	3	3	5
	0 -20	7	3	1	2

and also where VISST predicted 80-100% cloud for the ARSCL 0-20% bin (9% of cases). ARSCL's average cloud fraction was 29.5%, and VISST yielded an average cloud fraction 39.2% resulting in a bias of 9.7% with an RMS difference of 41.6%. At Manus, ARSCL and VISST cloud amounts agree 54% of the time within the limits of the bin range. Almost 42% of those cases were in the 80-100% cloud fraction bin reflecting the greater cloud fraction at Manus. The average ARSCL cloud fraction was 59.2%, 20.4% less than that from the VISST. The RMS difference is 44.2%.

A comparison of daytime ARSCL and GOES9 20-km radius averaged VISST cloud heights was made for Manus, and also for Nauru. The data were averaged according to cloud height classes based on ARSCL-detected cloud top height (zt): low clouds (ARSCL < 4 km), mid-level clouds (4 km <ARSCL < 7.5 km), and high-level clouds (ARSCL > 7.5 km). Further distinctions were made within these classes for cloud thicknesses (dz): thin cloud cases (ARSCL-detected *dz* < 1.5 km), medium *dz* (1.5 km - 3.5 km for mid- and high-level clouds, or 1.5 - 4.0 km for low clouds), and thick cases (*dz* > 3.5 km). Only cases having VISST-derived cloud amounts greater than 90% are examined here. Cloud cases are termed liquid if VISST classified at least 90% of the clouds as water. Likewise, they are defined as ice, if VISST defined at least 90% ice cloud.

Table 4a. Mean daytime cloud-top height (km) and thickness (km) from ARSCL and GOES-9 over Manus for high cloud amounts greater than 90%, April - September 2003.

ARSCL *dz* (km)	liquid 1.5 - 3.5	ice < 1.5	ice 1.5 - 3.5	ice > 3.5
N	3	12	36	135
ARSCL *zt*	14.2	12.5	12.7	12.3
VISST *zt*	9.4	11.6	11.0	11.7
zt rms	4.9	2.2	2.2	1.4
ARSCL *dz*	2.1	1.3	2.6	10.2
VISST *dz*	2.0	2.4	2.4	4.6
dz rms	0.7	1.6	0.9	6.2

Table 4b. Mean daytime cloud-top height (km) and thickness (km) from ARSCL and GOES-9 over Manus for mid-level cloud amounts greater than 90%, April - September 2003.

ARSCL *dz* (km)	liquid > 3.5	ice < 1.5	ice 1.5 - 3.5	ice > 3.5
N	1	1	5	8
ARSCL *zt*	5.5	4.4	6.4	6.0
VISST *zt*	2.3	9.8	10.7	9.8
zt rms	n/a	n/a	4.7	4.3
ARSCL *dz*	5.4	1.0	2.1	5.7
VISST *dz*	0.9	4.8	3.0	2.7
dz rms	n/a	n/a	1.2	3.4

The Manus high-cloud category (Table 4a), containing all available single-layer cases from April – September 2003, contained most of the cases (166). Fairly good agreement was found for the ice clouds. In thin ice cloud cases, the GOES-9 average *zt* was 11.6 km versus 12.5 km for ARSCL. For medium thickness cases, the VISST cloud top was 11.0 km, 1.7 km less than that from the ARSCL. The agreement is best for the thickest cases, with VISST *zt* averaging 11.7 km and ARSCL averaging 12.3 km. However, for the three water cases, the *zt* agreement is not as good. The medium thickness ARSCL cloud top is 14.2 km versus 9.4 km for VISST. This difference is most likely due to the presence of a thin cirrus cloud over a thick water cloud resulting in VISST classifying the cloud as water. Most of the radiance signal observed by GOES-9 would be due to the lower cloud. The cloud thicknesses derived from the VISST are too large for thin clouds and too small for thick clouds.

Table 4c. Mean daytime cloud-top height (km) and thickness (km) from ARSCL and GOES-9 over Manus for low cloud amounts greater than 90%, April - September 2003.

ARSCL *dz* (km)	liquid < 1.5	liquid 1.5 - 4	ice < 1.5	ice 1.5 - 4
N	2	3	3	7
ARSCL *zt*	3.1	2.9	1.5	3.1
VISST *zt*	3.4	2.9	12.9	11.9
zt rms	0.3	0.4	11.4	8.9
ARSCL *dz*	1.1	2.4	1.3	2.6
VISST *dz*	0.8	1.0	4.1	4.6
dz rms	0.3	1.6	3.1	2.2

Table 5. Mean daytime cloud-top height (km) and thickness (km) from ARSCL and GOES-9 over Nauru for cloud amounts greater than 90%, April - August 2003.

ARSCL *dz* (km)	high, ice <1.5	high, ice 1.5 - 3.5	low, water < 1.5	low, ice < 1.5
N	27	1	1	3
ARSCL *zt*	11.8	9.2	2.2	1.6
VISST *zt*	11.6	9.1	3.3	10.9
zt rms	1.6	n/a	n/a	9.3
ARSCL *dz*	0.8	1.6	0.1	0.2
VISST *dz*	2.3	1.3	0.8	2.8
dz rms	1.8	n/a	n/a	2.7

The agreement is not as good for the 11 medium-height cloud cases (Table 4b) over Manus. All of the VISST cases except one were classified as ice clouds. For the lone thin ice cloud case, the ARSCL-defined *zt* is 4.4 km while its VISST counterpart is 9.8 km. For the medium *dz* category, ARSCL determined the cloud tops at 6.4 km versus 10.7 km from VISST. Agreement for the thickest category is slightly better at 6.0 km for ARSCL and 9.8 km for VISST. For the lone thick liquid cloud case, agreement is still not very good. The ARSCL-defined the cloud top height as 5.5 km, and VISST determined it to be 2.3 km. In the ice cloud cases, it is possible that the differences are due to the lack of MMCR data at Manus; the GOES-9 infrared temperatures are not likely to be significantly colder than the temperature at cloud top for these optically thick cases. Further examination is necessary to determine the differences in the liquid water case.

For the low-level water clouds (Table 4c), the thin cloud comparison yields close agreement between the ARSCL *zt* (3.1 km) and the VISST *zt* (3.4 km). The RMS error and bias are both 0.3 km for this case. The medium thickness clouds agree almost exactly at 2.9 km, with an RMS difference of 0.4 km. However, for ice clouds, the cloud heights are substantially different. For thin cases, the VISST *zt* was 12.9 km versus 1.5 km for ARSCL, and for medium thickness clouds, the VISST cloud top height was placed at 11.2 km versus 3.1 km for ARSCL. Again, the lack of MMCR data to detect the upper level cloud probably causes the problems in the ice cases, as VISST cannot retrieve ice at the temperatures corresponding to cloud heights below 4 km in the Tropics.

The comparison of ARSCL and VISST-derived cloud heights for Nauru (Table 5) did not yield as many cases (N=44) as for Manus (N = 207). For the highest cloud levels (Table 4a), thin ice cloud heights show excellent agreement. On average, the ARSCL *zt* was 11.8 km, a value only 0.2 km higher than the VISST retrieval. The RMS difference is 1.6 km. The lone medium thickness high-cloud ice case is in good agreement: 9.2 km for ARSCL and 9.1 km for VISST. Only 32 of the Nauru cases are shown in Table 5; there were also two high thin water cloud cases (not shown) for which VISST averaged 11.1 km, 2.2 km less than ARSCL, and 10 mid-level cases. Like the Manus results, the mid-level cloud cases are not in good agreement (not shown), probably for the same reason noted earlier for the Manus site. For the low-level clouds, there was only one case of liquid thin cloud for which the ARSCL cloud top was at 2.2 km versus 3.3 km for VISST. For the ice cases (thin cloud), agreement is very poor presumably due to the lack of MMCR data.

4. DISCUSSION

A qualitative look at the GOES-9 VISST results indicates that the satellite retrievals are adequately capturing the spatial distribution of cloud features (e.g., Figs. 1a-d). Additionally, temporal trends, such as the higher summertime monsoonal cloud amounts in Darwin, are reproduced well. However, daily daytime averages are still questionable quantitatively because of some differences with the surface data that need further examination. In these cases, the differing methodologies and sampling areas for the three data sources may account for many of the differences in the cloud amounts.

To provide more accurate comparisons of daytime cloud amounts and heights at the three sites, the 20-minute averages of TSI and ARSCL properties were compared to 20-km radius GOES9 averages. Cloud amount differences for the 20-minute averages, while they are a better way to compare the values, are still influenced by the differing local environments. Although each site is coastal, the air-sea interactions peculiar to each site can be very different. At Nauru, a tiny island in a drier part of the domain, a low-level cloud plume is frequently created during the daytime, presumably by solar heating of the surface (Nordeen et al. 2001). The plume is frequently the only cloud in the vicinity and could greatly affect both the TSI and ARSCL cloud amounts at low cloud fractions as determined from GOES. Changes in wind direction have the plume often passing over the ARM site. Such plume behavior could explain the differences between GOES-9 and the surface cloudiness for cloud amounts below 30%. Other possible discrepancies in the cloud amount comparisons could be due to GOES-9 classifying partially-filled cloud pixels as entirely clear or cloudy, thus missing or overestimating some of the cloud cover viewed by the TSI.

From the matrix table cloud amount comparisons, it is not clear why ARSCL obtains lower cloud coverage than GOES-9 at Nauru. Overall the TSI and GOES9 derived values are in much better agreement. Perhaps, it is related to precipitation cases when the instruments are turned off; such effects need further examination. Visual inspection of the satellite imagery, for some of the cases where discrepancies occurred, reveals that broken clouds (common over the Nauru region), and possible sub-pixel scale clouds, could cause discrepancies in the cloud amounts between the two data sources. Additionally, some differences could be explained by the differences in fields of view sampled by each sensor; TSI views a different geometrical area than VISST, and the ARSCL cloud amount is derived from its narrow up-looking beam.

At Manus, the ARSCL, average cloud amounts are less than those from VISST by 20%. Manus is a larger landmass than Nauru and the ARM site is more on the windward side of the island compared to that at Nauru, where it is on the leeward side. Additionally, Manus is in an area where deep convection predominates, so that local effects may not be as important as over Nauru. The greatest differences are seen for small amounts of ARSCL-defined surface cloud cover (0-20%) with larger amounts from GOES-9 (21% of cases). At this point it is not possible to determine whether this is due to local effects, errors in the GOES-9 retrieval, or the effects of instrument downtime on the ARSCL analysis. For instance, some thin cirrus clouds detected by the MPL cannot be detected by the MMCR. If the MPL is not operating then such clouds could be missed by the MMCR. TSI data at Manus were only available from November 30, 2003- January 17, 2004. The comparisons of TSI versus GOES9 cloud amounts for this time period yielded better results than GOES9-ARSCL, albeit with a 10% bias.

ARSCL data are not currently available for the Darwin site. However, Darwin has the longest available time series of TSI data for comparison with GOES9, from May 2003- July 2004. The TSI cloud amounts are well correlated with the VISST results, but with some differences at lower cloud amounts. High clouds are not as predominant at Darwin as at Manus, so that the discrepancy could be due to differences in low cloud detection. Given the 20-km radius of the GOES-9 cloud fraction, it is possible that GOES-9 detects some low clouds that are essentially out of the Darwin TSI field of view. Since Darwin is located on the coast, it is possible that there is some sea-land breeze systematically producing low-level clouds in the vicinity that are often below the TSI horizon. This possibility should be examined using different averaging radii for the GOES-9 retrievals. Other sources of the discrepancies could be errors in the GOES-9 retrieval related to background reflectance and sub-pixel cloud cover.

GOES-9-derived cloud heights were compared with single-layer ARSCL clouds at both Manus (Table 3) and Nauru (Table 4). Cases were selected where both ARSCL and VISST-derived cloud amount exceeded 90%. Comparisons were made for thin, medium, and thick cases. In general, the daytime cloud heights between ARSCL and VISST compare well except for the cases that apparently lacked MMCR data to define the upper-layer cloud tops from the surface. The best agreement appeared to be for the low water and high ice cloud cases. In general, at Manus, the agreement is best for the thickest clouds, which are likely the most opaque thermally. For Manus, biases were -0.6 km for thick high ice cloud cases, (rms error 1.4 km), and -0.03 km for thickest low level water cloud (0.4 km rms error). Nauru had fewer cases overall (44) than Manus (207), and almost all were thin cloud cases. The best agreement was found for high thin ice clouds (27 cases) with a bias of -0.2 km and an rms error of 1.6 km.

5. SUMMARY AND FUTURE STUDIES

The VISST retrievals using GOES-9 data over the ARM TWP region are preliminary. However, the comparison of daytime cloud amounts with TSI- and ARSCL- derived cloud amount demonstrates that the VISST retrievals are relatively good, with daily averages revealing some differences that vary from site to site. Some of the differences are likely due to the various methods used to compute the cloud amounts. Differences may also be the result of field of view issues, such as clouds over the adjacent waters that are not measured by the surface instruments. Additional analyses of the differences should be undertaken to examine the sensitivity of the differences to averaging radius size and to the differences in clouds over the land and water parts of the averaging area. In addition to those sensitivity tests, errors of cloud misdetection by VISST will need to be evaluated. For example, improvement could be made by using more accurate determination of skin temperature for VISST's clear sky thresholding. To fully determine the scope of these differences, more comparisons with ARSCL-derived data, including nighttime cloud amounts, are needed.

Cloud heights, in general, seem to compare well with ARSCL-derived height if the phases agree. Most of the differences appear to be related to lack of MMCR data. However, further study of the datasets is required to ensure that this is source of the discrepancies. The GOES-9 derived cloud thicknesses, shown in Tables 4-5, were based on empirical functions determined over the ARM Southern Great Plains site. Comparisons with ARSCL-derived cloud thickness data indicate that new relationships should be derived specific to the ARM TWP region. Broadband shortwave albedos derived for the April - August 2003 time period agree well to those from CERES. Longwave flux validation remains for future work.

The results of these preliminary comparisons are encouraging and suggest that, at least for daytime, the GOES-9 data can be confidently used for model and process studies.

Acknowledgments

This research was supported by the U.S. Department of Energy Interagency Agreement DE-A102-97ER62341 and ITF No. 3407 from the Pacific Northwest National Laboratory. Some of the atmospheric profiles were generated by the CERES Meteorological, Ozone, and Aerosols group and obtained from the NASA Langley Atmospheric Sciences Data Center.

References

Chakrapani, V., D. R. Doelling, A. D. Rapp, and P. Minnis, 2002: Cloud thickness estimation from GOES-8 satellite data over the ARM SGP site. *Proc. 12th ARM Science Team Meeting*, April 8-12, St. Petersburg, FL, 14 pp. Available at http://www.arm.gov/docs/documents/technical/conf_0204/chakrapani-v.pdf.

Clothiaux, E. E., T. P. Ackerman, G. G. Mace, K. P. Moran, R. T. Marchand, M. Miller, and B. E. Martner, Objective determination of cloud heights and radar reflectivities using a combination of active remote sensors at the ARM CART sites, *J. Appl. Meteorol.*, *39*, 645-665, 2000.

Minnis, P., D. P. Kratz, J. A. Coakley, Jr., M. D. King, D. Garber, P. Heck, S. Mayor, D. F. Young, and R. Arduini, 1995: Cloud Optical Property Retrieval (Subsystem 4.3). "Clouds and the Earth's Radiant Energy System (CERES) Algorithm Theoretical Basis Document, Volume III: Cloud Analyses and Radiance Inversions (Subsystem 4)", *NASA RP 1376 Vol. 3*, edited by CERES Science Team, pp. 135-176.

Minnis, P., D. P. Garber, D. F. Young, R. F. Arduini, and Y. Takano, 1998: Parameterization of reflectance and effective emittance for satellite remote sensing of cloud properties. *J. Atmos. Sci.*, **55**, 3313-3339.

Minnis, P., P. W. Heck, and E. F. Harrison, 1990: The 27-28 October 1986 FIRE IFO Case Study: Cloud parameter fields derived from satellite data. *Mon. Wea. Rev.*, **118**, 2426- 2446.

Minnis, P., D. P. Kratz, J. A. Coakley, Jr., M. D. King, D. Garber, P. Heck, S. Mayor, D. F. Young, and R. Arduini, 1995a: Cloud Optical Property Retrieval (Subsystem 4.3). "Clouds and the Earth's Radiant Energy System (CERES) Algorithm Theoretical Basis Document, Volume III: Cloud Analyses and Radiance Inversions (Subsystem 4)", *NASA RP 1376 Vol. 3*, edited by CERES Science Team, pp. 135-176.

Minnis, P., L. Nguyen, D. R. Doelling, D. F. Young, W. F. Miller, and D. P. Kratz, 2002: Rapid calibration of operational and research meteorological satellite imagers, Part I: Evaluation of research satellite visible channels as references. *J. Atmos. Oceanic Technol.*, **19**, 1233-1249.

Minnis, P., W. L. Smith, Jr., D. P. Garber, J. K. Ayers,and D. R. Doelling, 1995b: Cloud properties derived from GOES-7 for Spring 1994 ARM Intensive observing period using Version 1.0.0 of ARM satellite data analysis program. *NASA RP 1366*, 58 pp.

Nguyen, L., D. R. Doelling, P. Minnis, and J. K. Ayers, 2004: Rapid technique to cross calibrate satellite imager visible channels. *Proc. SPIE 49th Ann. Mtg., Earth Observing Systems IX Conf.*, Denver, CO, August 2-6.

Nordeen, M. L., P. Minnis, D. R. Doelling, D. Pethick, and L. Nguyen, 2001: Satellite observations of cloud plumes generated by Nauru. *Geophys. Res. Lett.*, **28**, 631-634.

Trepte, Q., Y. Chen, S. Sun-Mack, P. Minnis, D. F. Young, B. A. Baum, and P. W. Heck, 1999: Scene identification for the CERES cloud analysis subsystem. *Proc. AMS 10th Conf. Atmos. Rad.*, Madison, WI, June 28 – July 2, 169-172.

Wielicki, B. A., et al., 1998: Clouds and the Earth's Radiant Energy System (CERES): Algorithm Overview. *IEEE Trans. Geosci. and Remote Sens.*, **36**, 1127-1141.